Report of the University of Oulu relating to the milestone "First application of improved detailed hydrological modelling linking groundwater and surface water in wetland restoration"

The effects of drainage and restoration on the hydrological processes of the Eenokinneva peatland: results from monitoring and HGS modelling in Freshabit Life project

Meseret W. Menberu, Anna-Kaisa Ronkanen, Hannu Marttila and Bjørn Kløve

Water, Energy and Environmental Engineering

University of Oulu

Finland

Abstract

In the Freshabit Life project (LIFE 14 IPE FI023), the impact of drainage and subsequent restoration on key hydrological processes of peatlands was analyzed analytically and numerically at previously disturbed, now restored Eenokinneva peatland (about 11.4 ha) located in Western Finland. The hydrological data collected included measurements of temporal and spatial water table (WT) depth within the peat layer (nine locations), runoff at the outlet and weather data (rainfall). The data included two years before restoration (drained condition) and one year after restoration (restored condition) during frost-free periods. Due to the unusual continuous dry rainfall-free periods observed in summer 2018, spotting the effect of restoration on the overall hydrological processes mathematically/analytically was difficult. However, during the relatively wet periods (May, October and November), the monthly mean WT after restoration at most of the WT measuring locations was at a higher depth (near to ground surface) than observed under drained condition (before restoration). Furthermore, event runoff coefficient before restoration was slightly higher than the value quantified after restoration. However, in 2018 (after restoration), due to several continuous dry and hot periods, there were less runoff event periods and longer monitoring is needed to confirm the effect of restoration on peatland hydrology. As a result, this study further used a three-dimensional fully integrated surface-subsurface hydrological modelling approach (HydroGeosphere) to overcome data limitations, unusual weather conditions and potentially detect disturbance-induced hydrological changes. We prepared a three-dimensional model that depict drained and restored conditions, and run the model in drained and restored conditions for each year in 2016, 2017 and 2018 using forcing weather data collected during frost-free periods. In all of the three rainfall conditions, runoff under drained conditions was significantly higher than simulated under restored conditions. The water table under restored conditions was significantly closer to the ground surface than simulated under drained conditions. The results obtained in Freshabit project have indicated possibilities of a three-dimensional surface-subsurface integrated model application in similar works in Finland and elsewhere.

The project has received funding from the LIFE Programme of the European Union. The material reflects the views by the authors, and the European Commission or the EASME is not responsible made of the information it contains.

1. Introduction

Peat is mainly composed of partially decomposed organic matter which forms when the rate of organic matter accumulation is far greater than microbial decomposition under favorable saturated moisture conditions (shallow or near to ground surface water table) (Holden et al., 2004). Peatlands are typically transitional zones between terrestrial and aquatic ecosystems, and play a vital role in regulating the hydrological, biogeochemical and ecological functions of the whole ecosystem (Joosten & Clarke, 2002; Krüger et al., 2015). Peatlands are complex ecosystems with unique characteristics but as transitional areas, peatlands could share some similar characteristics with terrestrial and/or aquatic ecosystems (Cherry, 2012). Some of the unique physical properties of peat include low bulk density, high total porosity, swelling and shrinking abilities during periods of wetting and drying (Dettmann et al., 2014). About 400 million ha (3% of the total land surface) of the global land surface area is covered with peatlands (Greenup et al., 2000; Joosten & Clarke, 2002). However, significantly large proportion of the global peatland resource (87%) is found in the northern hemisphere (Strack, 2008). In Finland, peatlands cover about one-third (9.15 million ha) of the total land surface area.

Globally peatlands are used for a variety of purposes. Peatlands under undisturbed conditions provide substantial ecosystem services through regulating the hydrological functions, ecological and biogeochemical processes; hence are essential habitats for unique biodiversity (Clarke & Rieley, 2010). Some of the hydrological and environmental benefits of peatlands are flood protection, groundwater recharge, stream flow maintenance, water purification and shoreline stabilization (Azous & Horner, 2000). Furthermore, peatlands sequester one-third of the global terrestrial carbon (about 600 gigatons of C) (Yu et al., 2011), hence play a vital role in mitigating climate change. Other benefits of peatlands include agriculture, forestry, peat-extraction for energy, recreation, and horticulture. However, some of the aforementioned benefits require land use and management changes; thereby modify the structure and function of peatlands. This could change peatlands from carbon sinks to sources and increase the global CO_2 emissions. A study of carbon emission from drained peatlands from 1990 to 2008 have reported a global CO2 emission increase by about 20% (Joosten, 2009). In Finland, nearly half of the total peatland area is used primarily for forestry and agricultural purposes and about 2% for energy production (Marttila & Kløve, 2010; Turunen, 2008).

Globally, about 14-20% of total peatland area (56-80 million ha) have been disturbed for a variety of human use, but primarily for forestry purposes (Strack, 2008). About 15 million ha of these disturbed peatlands are found in the boreal and temperate regions (Koskinen et al., 2011). From this, about 6 million ha of disturbed peatlands are located in Finland, which is roughly half of the total Finnish peatland area (Paavilainen & Päivänen, 1995), and are used primarily for forestry purposes. Hence, forestry-drainage is the major cause of peatland degradation in Finland (Haapalehto et al., 2011). Anthropogenic disturbance of peatlands alter the natural functions peatlands through its effect on hydrology (Menberu et al., 2016) and biogeochemical processes (Holden et al., 2004; Menberu et al., 2017). The immediate effects of peatland drainage is lowering of the water table, leaching of carbon, nitrogen and phosphorus to adjacent and downstream ecosystems (Menberu et al., 2017), thereby compromising water quality, aquatic fauna and flora. In Finland, there is a strong desire to ameliorate degraded peatlands through drain-blockage to re-establish the natural functions of peatlands. This was initiated manly due to; (1) the negative effects of peatland drainage, (2) failure to produce sufficient tree growth, and (3) Finland's strong desire and commitment to meet international and European agreements and conventions concerning biodiversity, water quality climate change.

For this study as a part of Freshabit Life project (LIFE 14 IPE FI023), the hydrology (water table depth and runoff) of previously drained, now restored peatland catchment (Eenokinneva peatland site) have been monitored both before (2016 and 2017) and after restoration (2018). Empirical analysis and numerical techniques (a three-dimensional fully integrated surface and subsurface hydrological model, Hydrogeopshere) were used to analyze the before and after hydrological regime changes at the Eenokinneva catchment. Hence, the main objectives of the study are to better understand the effects of catchment drainage and restoration: (1) on the runoff generation processes, (2) on catchment-scale water storage capacities and dynamics, and (3) on the spatial water table (WT) variations. Ultimate goal was to understand how peatland restoration change the hydrological processes in a catchment. Since the study was part of the Freshabit Life project focusing on methods and techniques to improve surface water qualities latter hydrological changes will be linked to the water quality data (peat water and runoff) collected from the Eenokinneva peatland.

2. Materials and methods

2.1. Study area

The study was carried out at the Eenokinneva peatland catchment (about 11.4 ha) located in Western Finland (Figure 1). The peatland is the part of Lauhanvuori National Park which includes also in Lauhanvuori-Hämeenkangas Geopark project. The Eenokinneva peatland area has been a unique mire with some groundwater discharging points nearby and in the eastern site of the area there are still some springs utilized for local households. The peatland site was drained for forestry during the 1970s with an average ditch depth and ditch width of 0.8 m and 1.5 m, respectively, and restored during the period 30 November to 6 December 2017. Distance between drainage ditches (ditch spacing) ranged from 30 m to 50 m (average 40 m). Parks & Wildlife Finland carried out the restoration operations as a part of their tasks in the Hydrology Life project (LIFE16 NAT/FI/000583). To block the ditches, peat-dams of length 6-10 m and height about 1 m were built across the ditches with spacing between the peat-dams ranging from 30 to 50 m. A 2-m × 2-m digital elevation model obtained from the National Land Survey of Finland used to delineate the study catchment boundary (Figure 1a). Long-term (1981-2010) annual mean air temperature and total precipitation from the nearby weather station (KANKAANPÄÄ NIINISALO PV, about 38 km far from the study site) is 4.1°C and 681 mm, respectively, (Pirinen et al., 2012).

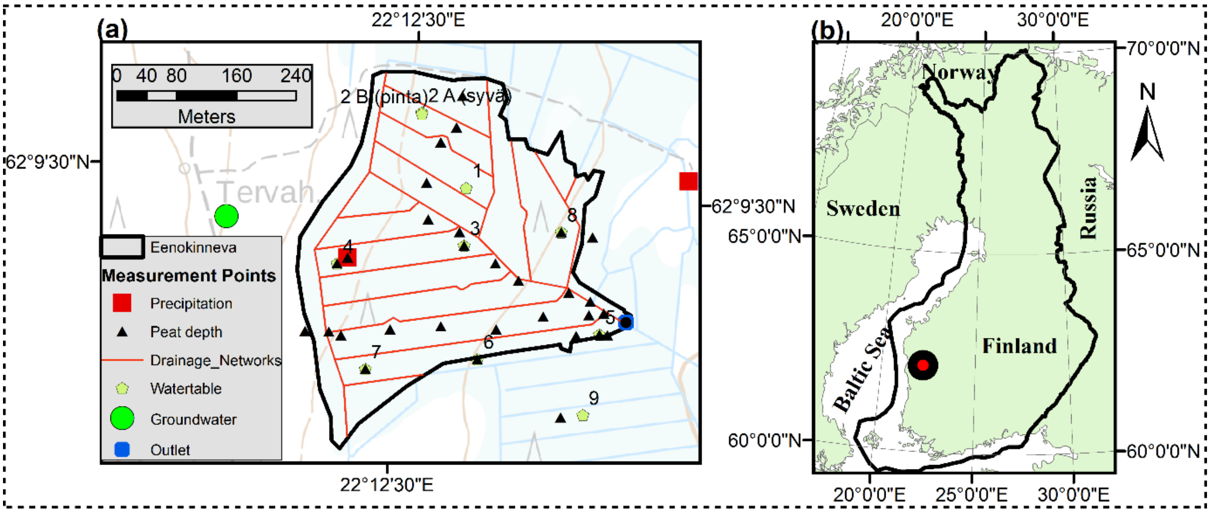

Figure 1. (a) The Eenokinneva peatland catchment study boundary and drainage networks with set up of hydrological monitoring (numbers indicate groundwater pipes used to monitor water table) and peat depth manual survey points, (b) location of the study site in Finland.

Typically, peat depth control water flow processes in peatlands, especially surface water groundwater interactions. To obtain a spatially representative peat depth of the studied Eenokinneva peatland, a manual peat thickness measurement campaign was carried out at 30 different locations within the peatland in 2017 (Figure 1). Furthermore, the ground penetrating radar (GPR) was done in 2018 to characterize the subsurface layer of the study area. Based on this survey, additional peat thickness data was extracted. Hence, both the manually measured peat thickness and GPR data used to generate peat depth raster for the entire study area using the kriging spatial interpolation technique in ArcGIS (Figure 2).

Peat depth varied from 0.10 m to 2.4 m (manual measurement) and 0.27 m to 2.4 m (from generated peat depth raster) (Figure 2). Soil core samples were taken by drilling to a depth of 11.5 m at the groundwater measuring location shown in the Figure 1. Drilling was done by South Ostrobothnia ELY center. Analysis of the soil core samples indicated the presence of sand (depth = 1 m), stone and gravel (depth = 1.6 m), gravel (depth = 6 m), till (depth = 7.2 m), gravel (depth = 8.8 m), mixture of rocks and gravel (depth = 9.5 m) and gravel (depth = 10.2 m). Furthermore, the estimated depth to bedrock from the ground surface is about 10.2 m. In-site falling-head direct push piezometer test for hydraulic conductivity (K) at different peat depths resulted in a significantly different K values between measurement depths (K = 2.60E-04 m/s at depth = 10 cm; K = 7.27E-05 m/s at depth = 20 cm; K = 4.84E-07 m/s at depth = 30 cm; K = 3.63E-08 m/s at depth = 40 cm; K = 4.24E-08 m/s at depth = 50 cm).

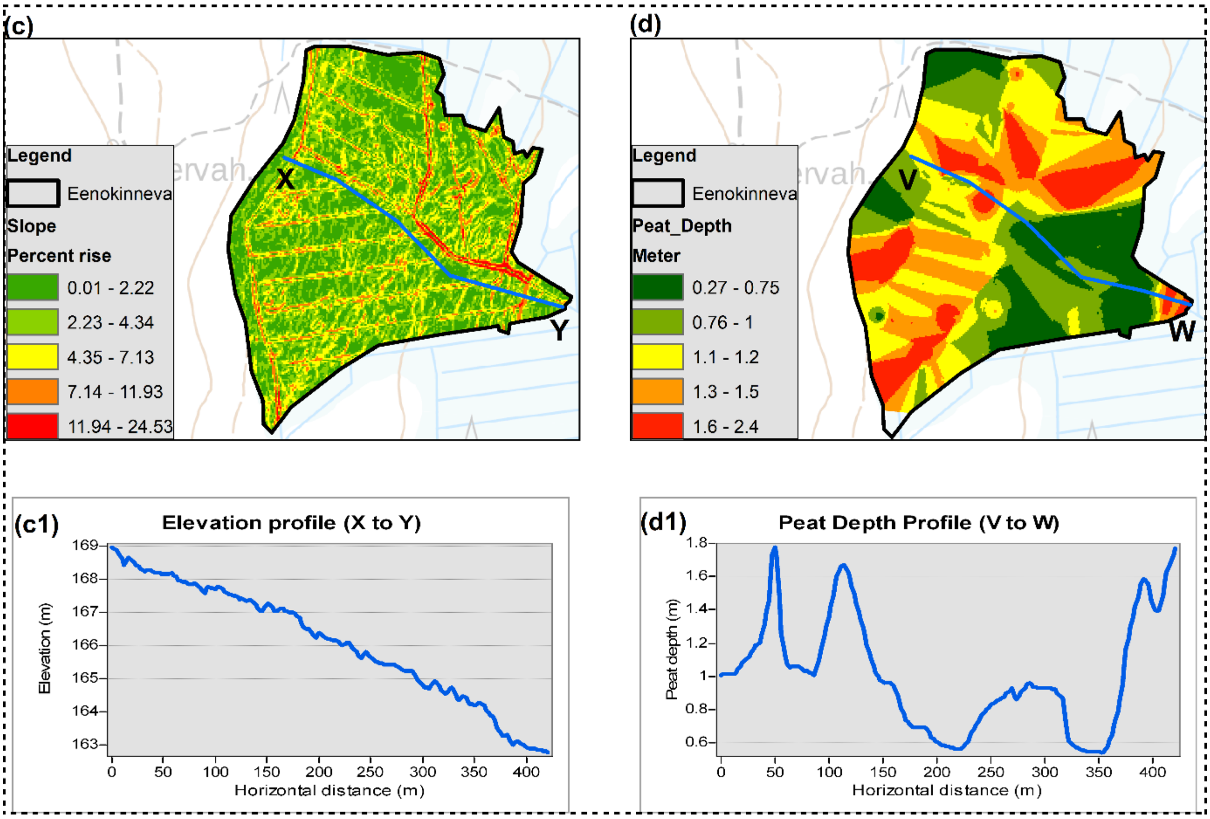

Figure 2. (c) The Eenokinneva peatland catchment slope (percent rise), (c1) surface elevation profile along the X, Y blue line, (d) peat depth raster in meters, and (d1) peat depth profile along V, W blue line in meters.

2.2. Hydrological data

High temporal resolution (1-hour interval) WT depth data in the peat layer at 10 locations (Figure 1,

Table **1**) were collected by installing a standpipe well of length 1-2 m and diameter 32 mm perforated from tip to center of the pipe. Each of the standpipe wells were equipped with automatic Solinst Levelogger that measure the barometric and water pressure. The barometric pressure was monitored using automatic Solinst Barologger and was used to compensate the data collected by the Solinst Leveloggers to get the WT level. Furthermore, the groundwater level at the upland mineral soil was monitored by drilling a well of about 11-m depth. Continuous runoff (Q) at the catchment outlet was measured by constructing a 90° V-notch equipped with Solinst Levelogger that measure the WL behind the weir (Figure 3). From this, the height of accumulation (h) was extracted to calculate Q in the power function shown in equation (5) (Koskinen et al., 2017; Menberu et al., 2018).

$$Q = 0.0142h^{2.5} \tag{1}$$

High temporal resolution rainfall (1-hour interval) data was collected using automated tipping bucket rain gauges at two locations (Figure 1) using Solinst rainlogger edge to log rainfall events. Due to malfunctioning of the rainfall monitoring equipment in 2018 and partly for 2016, daily rainfall data was obtained from a 10-km x 10-km gridded rainfall data provided by the Finnish Meteorological Institute.

Figure 3. The Eenokinneva peatland catchment runoff monitoring V-notch weir.

Table 1. Water table (WT) well locations' peat depth, distance to the closest ditch, surface elevation and distance to catchment outlet.

WT well	Peat depth (m)	Distance to ditch (m)	Distance to outlet (m)	Elevation (m)
1	1.61	9.80	280.00	167.00
2A	0.90	12.00	392.00	167.40
2B	0.90	12.00	392.00	167.40
3	0.57	16.50	240.00	166.99
4	2.13	15.50	395.00	168.82
5	1.21	16.60	40.00	163.00
6	0.40	10.50	205.00	165.28
7	2.20	18.00	355.00	167.67

8	0.75	23.00	149.00	165.11
9		15.00		163.33

2.3. Hydrological data analysis

2.3.1. Water table related hydrological changes

The WT residence time curves (plot of WT depth against probability of exceedance in percent time) were quantified for each WT well (Holden et al., 2015; Menberu et al., 2016). The WT residence curves were used to compare the spatial WT depth variability and the impacts of restoration on the WT depth. The probability of exceedance of a certain WT depth (also called WT residence time curves) for a given period has important practical implications. The exceedance probability provides important information about the chances of occurrence or exceedance of any required WT depth for a specified duration. The WT fluctuation method (WTF) shown in equation (5) was used to quantify the WT recharge (proxy for change in WT storage), and used to evaluate the WT storage change before and after restoration.

$$\Delta SWT = \mathrm{Sy}\frac{\Delta h}{\Delta t} = Sy(\Delta h1 + \Delta h2 + \Delta h3 + \Delta h4 \ldots + \Delta hn) \qquad (2)$$

Where ΔSWT is change in the WT storage (recharge), *Sy* is the specific yield, Δh is the change in WT depth (difference between peak of WT rise and low point of the projected antecedent WT decline at the time of the peak WT, Figure 4) and *t* is time. The basic assumption to this approach is that, the water reaching the WT goes to storage and other components of the WT budget (e.g., base flow, evapotranspiration and net subsurface flow) are set to zero at the time of recharge (Healy & Cook, 2002). Hence, the WTF method is most appropriate when used over short period (e.g., hours or few days). However, this method could overestimate recharge values as it may include WT rises unrelated to recharge. Furthermore, the WTF method requires estimation of the *Sy* at the depth of WT fluctuation. The average *Sy* of the studied peatland area at the depth of WT fluctuation was estimated using the water balance equation written as in equation (5).

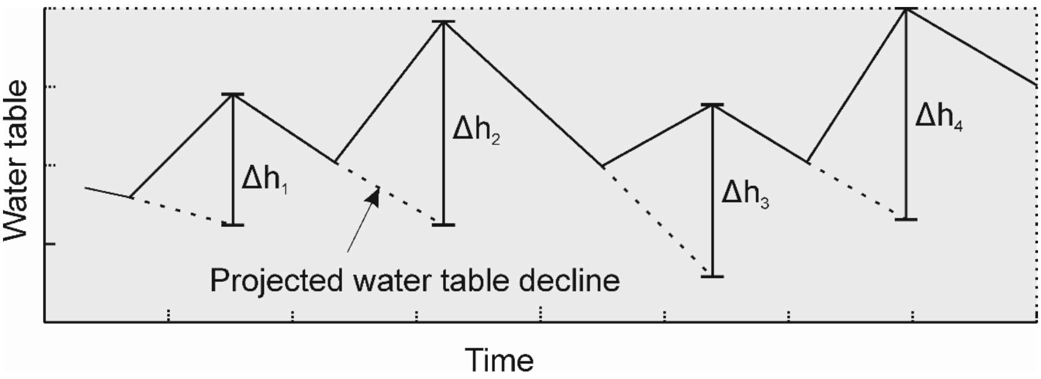

Figure 4. The Master Recession Curve approach to quantify the change in water table height to estimate recharge using the water table fluctuation method.

$$\mathrm{Sy} = \frac{P + Q_{in} - ET - Q_{out}}{\Delta h} \tag{3}$$

Where P is rainfall, Q_{in} is inflow (Q_{in} was assumed to be zero), ET is evapotranspiration (daily ET about 1.52 mm/day assumed, (Wu et al., 2010)), Q_{out} is runoff and Δh is WT rise.

The amplitude of WT fluctuation (AWTF) was quantified for each WT measuring well using equation (5) (Azous & Horner, 2000; Menberu et al., 2016). To evaluate the significance of anthropogenic disturbance on WT properties, the estimated amplitude of WT fluctuation at each WT measuring well was compared using analysis of variance (one-way ANOVA with post hoc test).

$$AWTF_i = WTmax_i - 0.5(WTmin_i + WTmin_{i-1}) \tag{4}$$

where $AWTF_i$, $WTmax_i$, and $WTmin_i$ are the amplitude of WT fluctuation, maximum WT depth, minimum WT depth at sampling occasion i, and $WTmin_{i-1}$ is the minimum WT depth at sampling occasion i-1. Furthermore, basic descriptive statistics of the WT depth at each measuring well quantified on weekly and monthly basis. These values were compared for statistically significant differences (one-way ANOVA with post hoc test) at a probability level of $P = 0.05$ between WT measurement locations (spatial WT variation), before and after restoration. The impact of restoration on the mean WT depth at each measuring location was evaluated by calculating

Cohen's effect size (Cohen's d) using equation (5). Furthermore, the effects of peat depth, WT well distance to nearest ditch, WT well distance to outlet weir and WT well surface elevation (

Table **1**) on the WT depth were tested using Pearson's correlation analysis.

$$\text{Cohen's d} = \frac{MeanWT_{BR} - MeanWT_{AR}}{\sigma_{pooled}} \qquad (5)$$

where $MeanWT_{BR}$, $MeanWT_{AR}$ is mean WT before restoration and after restoration, respectively, and σ_{pooled} is the pooled standard deviation.

2.3.2. Runoff characteristics

To measure the response of the *Eenokinneva* peatland catchment for a given rainfall input, runoff hydrograph events were selected both before and after restoration. To measure the effect of restoration on catchment response, event-based runoff characteristics (runoff coefficient, peak flow, hydrograph base time and time to peak runoff) were quantified from selected event runoff hydrographs. The effect of restoration on the base flow was analyzed by selecting runoff during no rainfall periods and by constructing the flow duration curves. Furthermore, to understand the runoff generation processes both before and after restoration, event runoff characteristics and base flow were analyzed against the WT fluctuation (antecedent WT and WT during the event) using Pearson's correlation analysis.

2.4. Numerical methods

The HydroGeoSphere, a three dimensional fully integrated surface-subsurface hydrological modelling code (Aquanty, 2015) was used to solve the effect of artificial drainage and subsequent restoration on the hydrology of the *Eenokinneva* peatland catchment. A 2-D mesh with 3-node triangular elements, which was highly refined along the drainage networks, was first generated for the ground surface using GRIDBUILDER (Brunner & Simmons, 2012; McLaren, 2004). Before restoration, the drainage networks were represented by v-shaped channel (1.5 m width on the surface and 1 m depth) by adjusting the elevations of the longitudinal profile of each ditch using Tecplot software (Tecplot, 2013) and ditch beds were smoothed to lower computational complexity. Furthermore, to mimic the site condition after restoration, several dams (width of dam 5 to 10 m and distance between dams about 40 m) across the drainage networks were created by modifying the elevation of the longitudinal profile of each drainage channel using Tecplot software. Consequently, the 2-D mesh created at GRIDBUILDER was exported to suitable file format to create the three-dimensional model in HydroGeoshere. The model domain (Figure 5) contained seven vertical finite element layers (146744 nodes, 255206 elements), in which each finite element has triangular prismatic-shape with 6-nodes. An average peat depth of 1.10 m was used in the model and was discretized into three distinct layers with 0.2 m, 0.4 m and 1.1 m depth below ground surface. Underneath the bottom peat layer at 2.6 m below ground surface is the sand layer. The till layer, which is found between the sand and the bedrock (10.2 m below ground surface) is discretized into three layers (Figure 5). The HydroGeoSphere uses the 2-D depth-averaged diffusion-wave approximation of the Saint Venant equation to solve the surface flow and Richard's equation to solve the saturated/unsaturated subsurface flow. For detail description of the equations and processes involved in solving the complex surface and subsurface hydrological model, please refer to the HydroGeosphere manual (Aquanty, 2015).

In the bottom of the model domain (bedrock surface), a no flow boundary condition was assigned, specified head boundary condition around the perimeter of the porous media domain and critical depth boundary condition around the perimeter of the surface domain was assigned. Furthermore, model parameters are provided in Table 2 and evapotranspiration parameters are taken from other published research work (Ala-aho et al., 2015). Firstly, the model was run into a steady state by using effective annual rainfall amount of 315 mm to get an initial condition for individual transient run for years 2016, 2017 and 2018. The observed runoff and WT measured at the center of the study site (Well_1) were used to calibrate some of the model parameters (e.g., Manning's roughness coefficient, obstruction and rill storage height). Hence, the transient model was run for summer periods of year 2016, 2017 and 2018 for both drained and restored conditions. As a result, the effect of anthropogenic disturbance can easily be compared under similar forcing climatic conditions.

Table 2. Model parameters used that differ from the default parameter values of the HydroGeosphere model. Data sources (Ala-aho et al., 2015; Li et al., 2008; Schwarzel et al., 2006), hydraulic conductivity of peat was measured on-site.

Model domain	Parameter	Peat			Sand	Till
		Depth below surface				
Porous media		0.20 m	0.40 m	1.10 m		
	Hydraulic conductivity (m s^{-1})	7.27E-5	2.6E-7	3.63E-8	4E-4	5E-5
	Porosity	0.92	0.86	0.86	0.43	0.37
	Specific storage (m^{-1})	1E-1	1E-1	1E-1	4.92E-5	1.6E-4
	vG residual saturation	0.058	0.058	0.058	0.043	0.12
	vG α (m^{-1})	2.5	0.19	0.57	2.35	2.8
	vG β	1.14	1.25	1.16	2.38	1.9
	Minimum relative permeability	1E-11	1E-11	1E-11	1E-9	1E-9
Overland media		Peat	Channel			
	Manning's n ($m^{-1/3}s$)	0.6	0.04			
	Rill storage height (m)	0.2	0.01			
	Obstruction storage height (m)	0.2	0.001			
	Coupling length (m)	0.01	0.01			

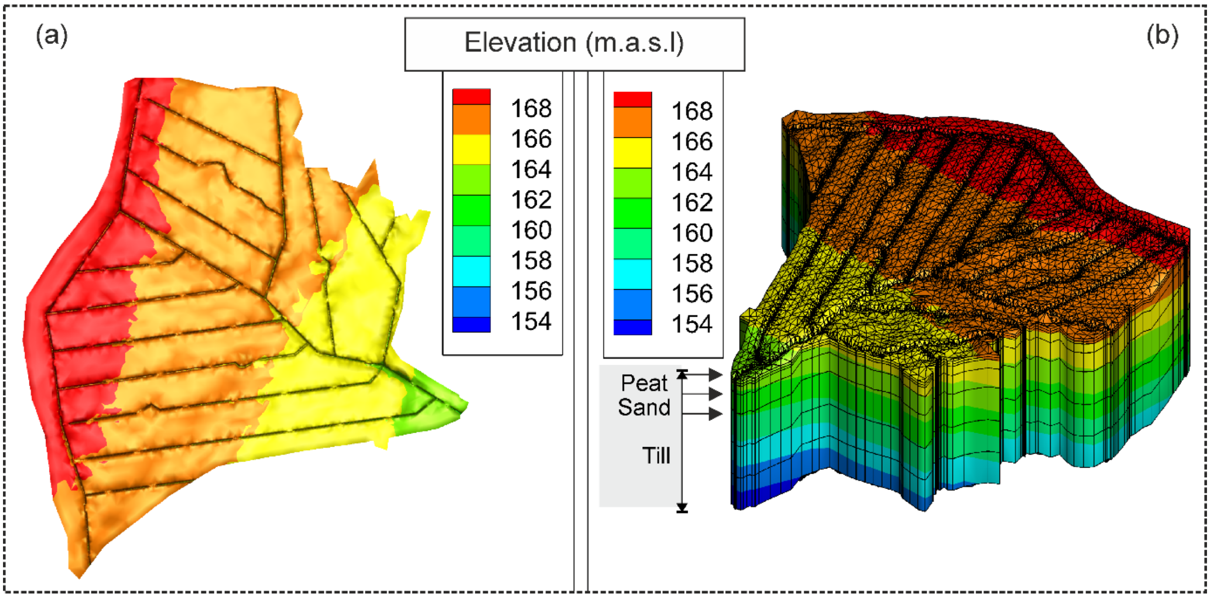

Figure 5. (a) Overland flow domain showing the artificial drainage ditch networks (b) configuration of the finite element mesh of the Eenokinneva catchment showing hydrostratigraphic units. For restored condition, the elevation of the longitudinal profile of each drainage channel raised to an elevation by about 0.1 m higher than the ground surface.

3. Results and discussion

3.1. Hydrological data analysis

3.1.1. Water table dynamics

The aggregated mean WT before restoration (mean ± SD; -24.7 ± 18.0 cm below peat surface) was significantly deeper (one-way ANOVA; $p < 0.05$) than the after restoration (mean ± SD; -21.3 ± 17.8 cm below peat surface). However, this was evident only at well_2A (Cohen's d = 1.4) and well_6 (Cohen's d = 1.97). The effect of restoration on the WT depth was clearly visible at all wells during wet periods (May, October and November), in which the mean monthly WT depth was at shallower depth than the condition observed before restoration. However, except at well_2A and well_6, due to extreme hot summer conditions during June, July and August 2018, the mean monthly WT after restoration for the rest of the wells was fluctuating at depths deeper than before restoration (Figure 6).

The WT level at the center of the Eenokinneva catchment (well_1 and well_3) and upstream (2A and 2B) fluctuated within 0 to 40 cm of the surface for most of the study period both before and after restoration (Figure 7). Irrespective of the rainfall amount, the WT level after restoration fluctuated at depth shallower than before restoration at location well_2A, well_2B, well_3, well_4 and well_6 for most of the study period. However, for about 30 % of the study period, WT level after restoration fluctuated at depths deeper than before restoration at most of the WT measuring locations. This was partly due to the unusual occurrence of continuous drier and hotter days in summer 2018 than observed in 2016 and 2017. The Finnish Meteorological Institute reported that summer 2018 was among the top ten hottest years ever recorded. The highest temperature was 33.7°C, recorded on 18 July in Klemettilä, Vaasa (Finnish Meteorological Institute, 2019) about 130 km far from the Eenokinneva catchment.

The difference of the mean AWTF of the WT level before and after restoration at each measuring location was not significantly different, except for well_9, which is located outside of catchment area. Except at well_2B, well_5 and well_6, the mean AWTF after restoration for the rest of WT measuring locations was slightly higher than before restoration (Figure 8). However, analysis of the aggregated WT of all measuring locations, the mean AWTF before restoration was slightly higher (but not significant) than the after restoration. The upland mineral soil groundwater had significantly smaller AWTF than observed in the peatland area.

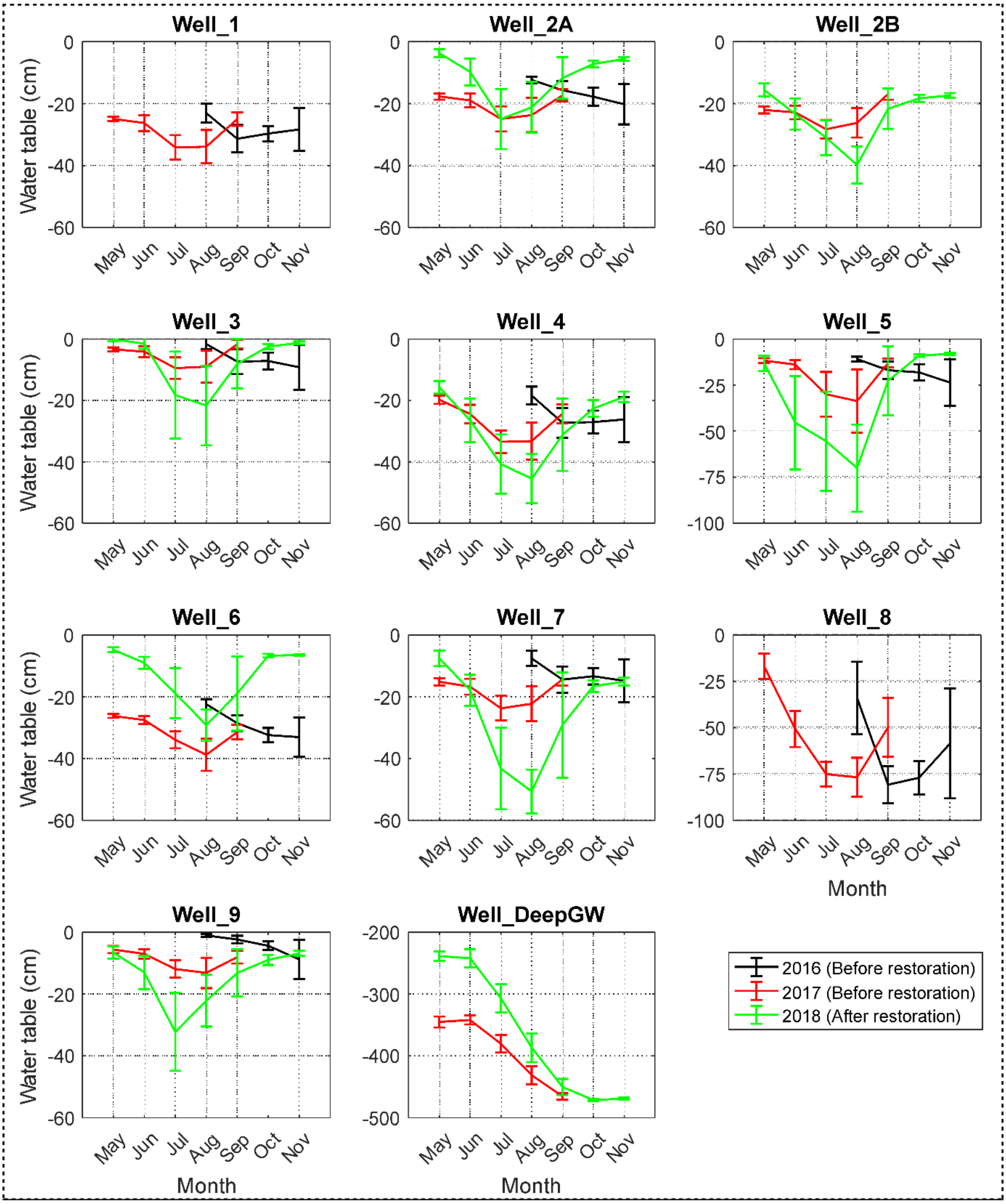

Figure 6. Monthly mean water table plots for each water table measuring spot and upland mineral soil groundwater (well_DeepGW) before restoration (2016 and 2017) and after restoration (2018). Bars show standard deviation.

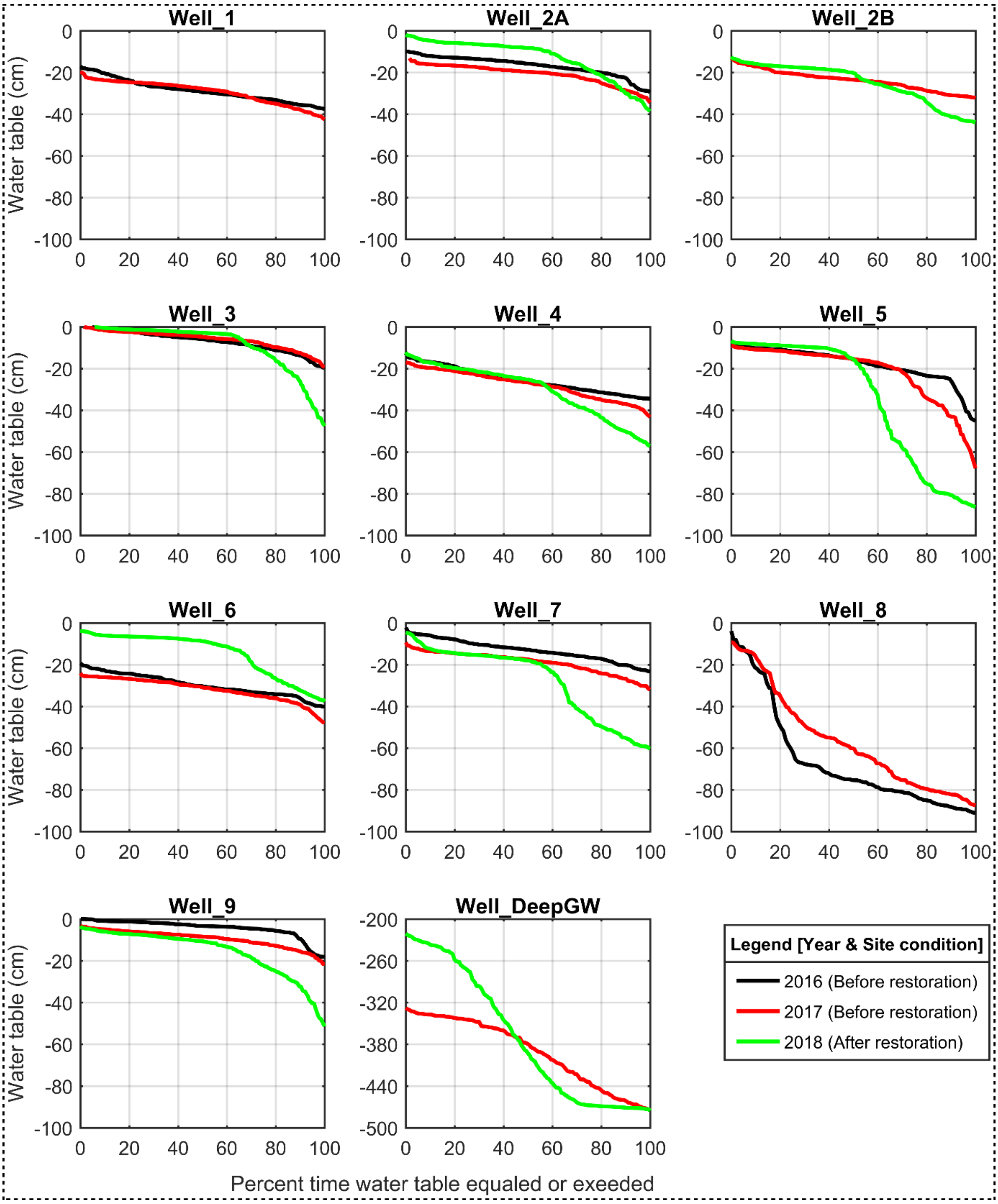

Figure 7. Water table depth duration curves for each water table measuring well. Negative water table represents depth below ground surface and for upland mineral soil groundwater (well_DeepGW).

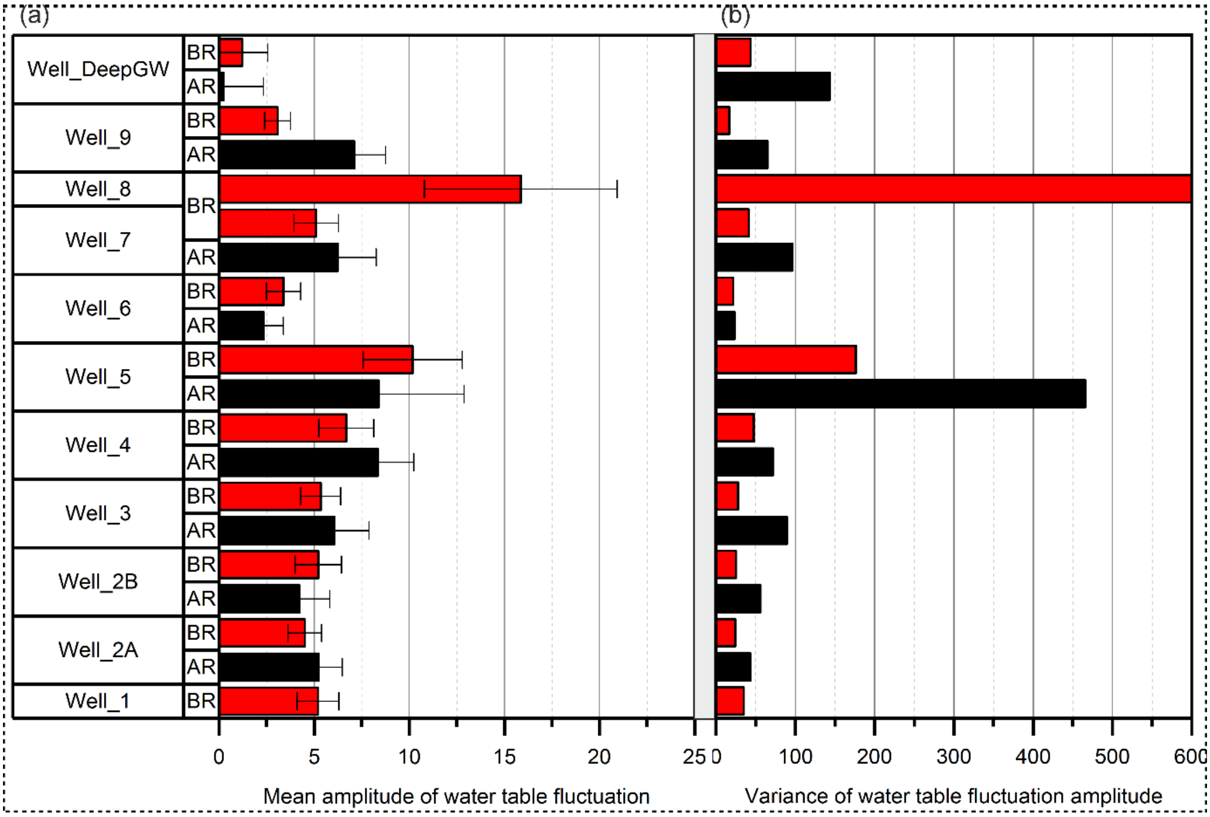

Figure 8. (a) the mean and standard error of mean of the water table fluctuation amplitude, (b) variance of the water table fluctuation amplitude at each water table measuring location before restoration (BR) and after restoration (AR), and for upland mineral soil groundwater (well_DeepGW).

The WT depth was deeper near to the ditch than observed at a farther distance from the nearest ditch as revealed by Pearson's correlation analysis between WT depth and distance to nearest ditch (Pearson’s r = 0.36). The WT depth showed negative correlations with peat surface elevation (Pearson’s r = –0.21) and peat depth (Pearson’s r = –0.48). Furthermore, the peat depth correlated positively with distance to ditch (Pearson’s r = –0.41), distance to outlet weir (Pearson’s r = –0.33) and peat surface elevation (Pearson’s r = –0.42).

3.1.2. Interaction of the peatland with rainfall and other climatic factors

The mean Sy estimated for the aggregated data before restoration (Sy ranged from 0.03 to 0.49) was slightly higher but not significantly different from that of the after restoration (Sy ranged from

0.03 to 0.61). The Sy estimated at each WT measuring spot before and after restoration was not statistically different (Table 3). Except for well_3 and well_5, the Sy values estimated before restoration for the rest of the wells was slightly higher than the after restoration. The Sy correlates significantly with the minimum WT (Pearson's $r = 0.50$) and maximum WT (Pearson's $r = 0.21$) of the selected rainfall induced WT fluctuation events. Regression analysis further revealed that the Sy significantly varied when the WT fluctuated within 30 cm from the surface of the peat (Figure 9).

Table 3. The specific yield values for each water table measuring location and aggregated data estimated using the water balance equation. SEM is standard error of the mean. $p > 0.05$ indicates the difference is not statistically significant.

Wells	Before restoration				After restoration				ANOVA
	Mean	SEM	Minimum	Maximum	Mean	SEM	Minimum	Maximum	*p*
Well_1	0.18	0.02	0.09	0.29	-	-	-	-	
Well_2A	0.19	0.03	0.07	0.41	0.15	0.04	0.06	0.34	0.37
Well_2B	0.19	0.02	0.13	0.29	0.16	0.02	0.09	0.23	0.39
Well_3	0.20	0.04	0.08	0.38	0.21	0.09	0.05	0.61	0.85
Well_4	0.15	0.01	0.07	0.24	0.12	0.03	0.04	0.32	0.34
Well_5	0.14	0.04	0.03	0.46	0.15	0.08	0.03	0.42	0.87
Well_6	0.26	0.04	0.14	0.49	0.26	0.12	0.11	0.61	0.95
Well_7	0.18	0.03	0.08	0.38	0.14	0.03	0.06	0.33	0.39
Well_8	0.09	0.02	0.03	0.19	-	-	-	-	
Well_9	0.19	0.02	0.11	0.30	0.14	0.03	0.05	0.31	0.19
Aggregated	0.17	0.01	0.03	0.49	0.16	0.02	0.03	0.61	0.41

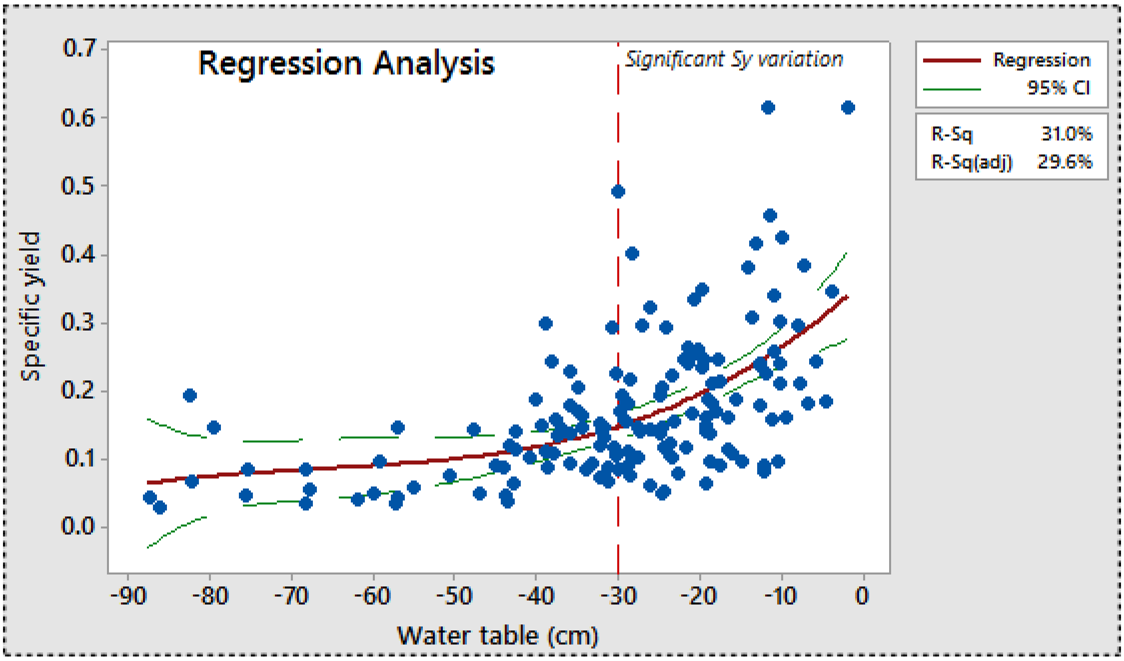

Figure 9. Regression analysis between the rainfalls induced aggregated water table fluctuation data from all wells and associated specific yield estimates.

The peat water interaction referred here as recharge (change in storage of the saturated zone) of the aggregated WT data before restoration (mean recharge rate = 0.61 cm/day) was significantly higher than the after restoration (mean recharge rate = 0.41 cm/day). Except for well_2B, the recharge rate before and after restoration for the remaining WT measuring locations was not significantly different. However, the mean rate of recharge before restoration was higher than the after restoration (except for well_2A) as also reflected by the recharge coefficient (Figure 10).

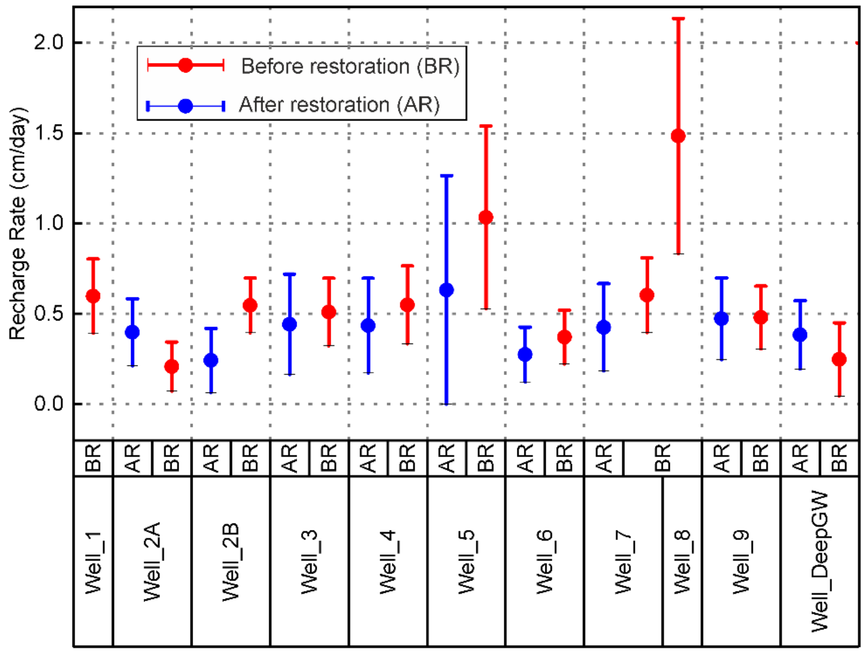

Wells	Recharge Coefficient BR	Recharge Coefficient AR
Well_1	0.94	-
Well_2A	0.33	0.69
Well_2B	0.62	0.42
Well_3	0.80	0.77
Well_4	0.86	0.75
Well_5	1.62	1.09
Well_6	0.58	0.48
Well_7	0.95	0.74
Well_8	2.33	-
Well_9	0.75	0.82
DeepGW	0.28	0.66

Figure 10. Peat water interaction shown as recharge rate (mean and 95 % confidence interval of the mean) for each water table measuring location and upland mineral soil groundwater (DeepGW), and associated recharge coefficient before restoration (BR) and after restoration (AR).

3.1.3. Runoff characteristics and interaction with water table

The number of rainfall induced runoff events selected were few both before restoration (5 events) and after restoration (4 events) due to short-term study period (Table 4). Hence, with consideration being given to that, the runoff coefficient (RC) quantified before restoration (mean ± SEM = 0.19 ± 0.03) was higher (but not significantly) than after restoration (mean ± SEM = 0.17 ± 0.09). Although not statistically significant, the peak flow intensity (PFI) after restoration (mean ± SEM = 0.03 ± 0.01 l/s/mm) has also been reduced by half when compared to the PFI calculated before restoration (mean ± SEM = 0.07 ± 0.03 l/s/mm).

Table 4. Rainfall-induced runoff events and associated runoff properties, runoff coefficient (RC), hydrograph intensity (PFI; peak flow intensity normalized by total rainfall).

Event	Start date	End date	Total rainfall (mm)	Net rainfall (mm)	RC	PFI (l/s/mm)
Before restoration						
Event_1	20/6/2017	30/6/2017	44.20	32.20	0.20	0.064
Event_2	3/7/2017	7/7/2017	10.00	5.20	0.12	0.075
Event_3	28/7/2017	8/8/2017	38.60	25.40	0.12	0.034
Event_4	28/8/2017	4/9/2017	35.00	26.60	0.25	0.104
Event_5	8/9/2017	19/9/2017	30.60	17.40	0.26	0.052
After restoration						
Event_1	17/9/2018	2/10/2018	27.70	9.70	0.07	0.008
Event_2	4/10/2018	11/10/2018	15.30	6.90	0.15	0.040
Event_3	21/10/2018	28/10/2018	11.00	2.60	0.28	0.028
Event_4	2/11/2018	5/11/2018	5.70	2.10	0.17	0.048

There were several occasions where the base flow after restoration remained insignificant during rainfall-free periods when compared to the condition before restoration (Table 5, Figure 12). The base flow calculated before restoration (mean ± SEM = 0.93 ± 0.04 mm/day) was significantly higher (one-way ANOVA; $p < 0.05$) than after restoration (mean ± SEM = 0.0083 ± 0.001 mm/day). This could be one of the immediate effects of restoration until the available space for storage is filled with incoming water. Another study on restored peatland sites that comprised four years of data after restoration reported a mean base flow of 0.8 mm/day (Menberu et al., 2018) indicating the base flow at the Eenokinneva catchment could eventually increase when the available space for storage created by drain-blockage is filled over time. Furthermore, the flow duration curve revealed that before restoration higher peak flow and sustained base flow conditions occurred than observed after restoration (Figure 11). Before restoration, runoff and base flow seemed to occur when depth to water table was below 30 cm from the surface unlike the condition after restoration (Figure 12).

Table 5. Rainfall-free period mean runoff (base flow; BF) property of the *Eenokinneva* catchment for each rainfall-free occasion.

Before restoration				After restoration			
Occasion	Start date	End date	BF (mm/day)	Occasion	Start date	End date	BF (mm/day)
BF_1	12.5.2017	16.5.2017	1.73	BF_1	18.5.2018	5.6.2018	0.00
BF_2	19.5.2017	26.5.2017	1.36	BF_2	9.6.2018	14.6.2018	0.00
BF_3	15.6.2017	17.6.2017	0.65	BF_3	25.6.2018	27.6.2018	0.00
BF_4	30.6.2017	2.7.2017	0.48	BF_4	30.6.2018	1.7.2018	0.00
BF_5	26.7.2017	27.7.2017	0.13	BF_5	7.7.2018	11.7.2018	0.00
BF_6	23.8.2017	24.8.2017	0.03	BF_6	15.7.2018	19.7.2018	0.00
BF_7	3.9.2017	6.9.2017	0.46	BF_7	23.7.2018	28.7.2018	0.00
				BF_8	8.8.2018	9.8.2018	0.00
				BF_9	15.8.2018	16.8.2018	0.00
				BF_10	30.8.2018	31.8.2018	0.00
				BF_11	3.9.2018	6.9.2018	0.00
				BF_12	1.10.2018	2.10.2018	0.14
				BF_13	13.10.2018	14.10.2018	0.04
				BF_14	27.10.2018	29.10.2018	0.05

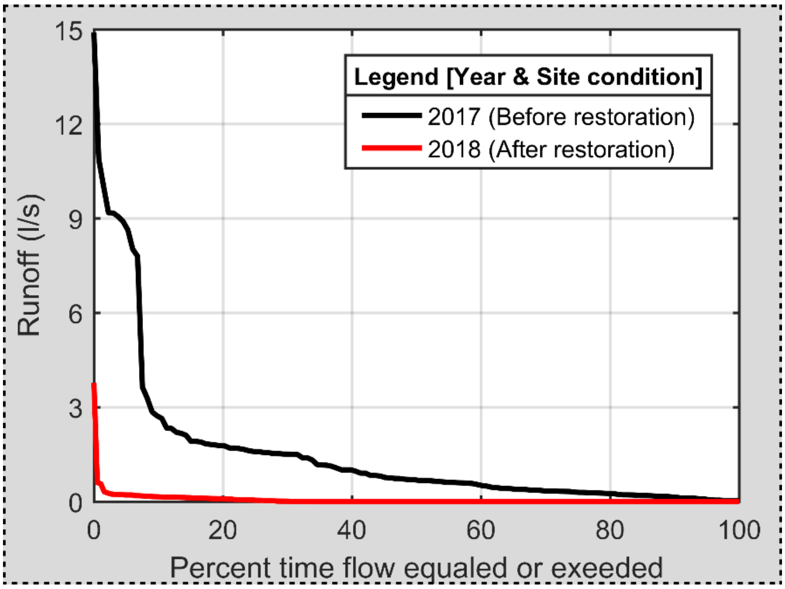

Figure 11. Flow duration curves for the Eenokinneva study catchment before (2017) and after restoration (2018).

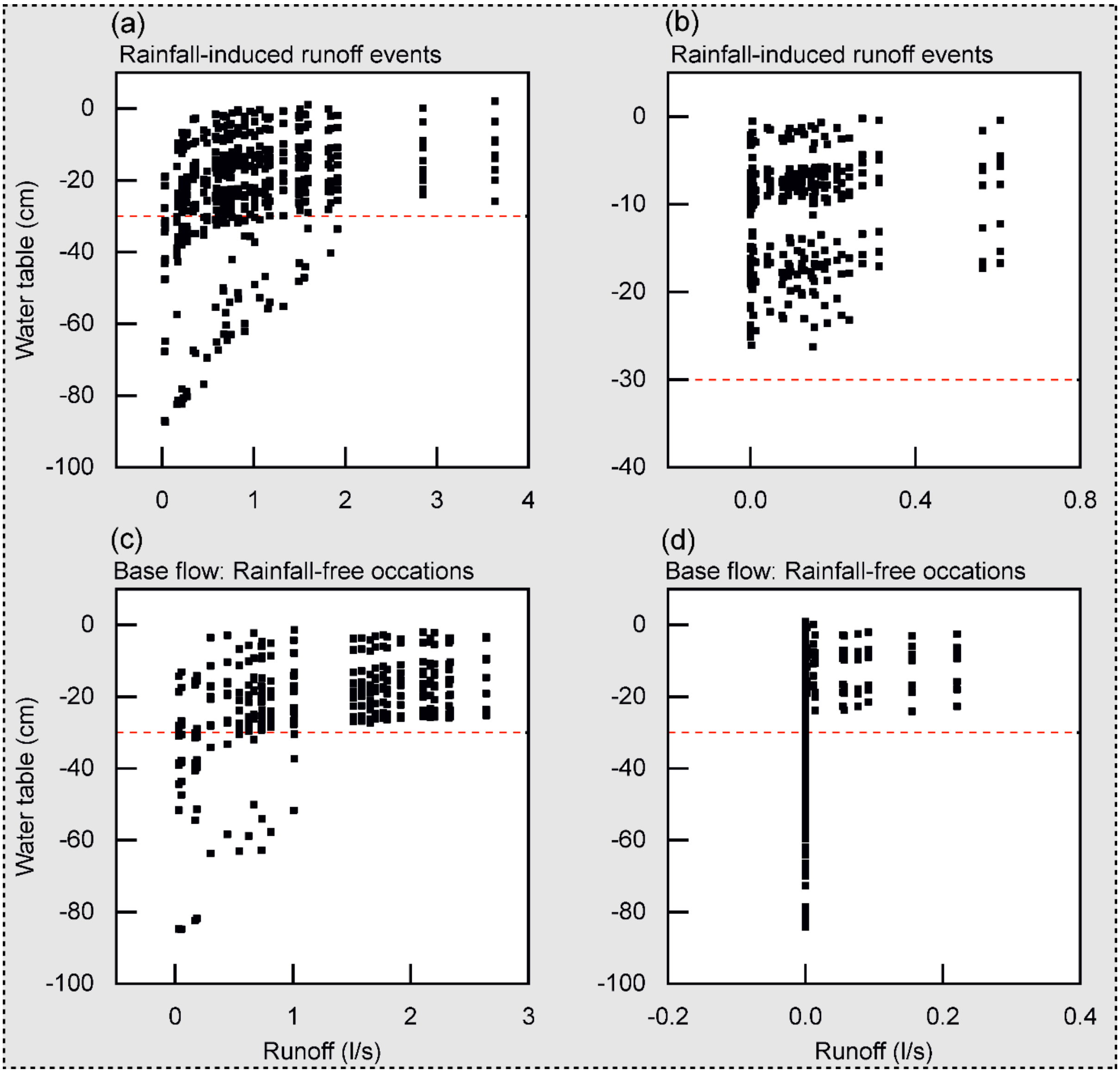

Figure 12. Runoff and water table relationship before restoration (a, c) and after restoration (b, d) during rainfall (rainfall-induced runoff) and rainfall-free periods (base flow). Red horizontal line shows depth to water table where runoff and base flow varies significantly.

Furthermore, the runoff generation process during rainfall-free periods (base flow) showed positive correlation with WT fluctuation measured at different spots, however, the correlation was significant with WT fluctuation measured at well_3 (Pearson's r = 0.22), well_4 (Pearson's r = 0.44), well_5 (Pearson's r = 0.41), well_7 (Pearson's r = 0.29) and well_9 (Pearson's r = 0.42). The runoff generation during rainfall periods also showed significant relations with the WT fluctuation measured at well_3 (Pearson's r = 0.33), well_4 (Pearson's r = 0.28), well_7 (Pearson's *r* = 0.45), well_9 (Pearson's *r* = 0.52) and with groundwater measured at upland mineral soil (Pearson's *r* = 0.47).

3.2. Numerical methods

3.2.1. Model calibration

The measured surface runoff and WT data measured at the center of the *Eenokinneva* catchment (well_1) in summer 2017 before restoration were compared to the simulated hydrological data to evaluate the model efficiency. Some model parameters were calibrated manually (trial-and-error) to get better model performance (better fit) and model calibration run typically avoided hydrological data measured during May to minimize the effect of winter processes, e.g., snowmelt (due to lack of data and primary objective of the research, snowmelt was not considered in the model) in the model efficiency. The model produced satisfactory fit between measured and simulated hydrological data as the Nash-Sutcliffe efficiency (NSE) indicated (Figure 13). The model overestimated the peak flow; however, the runoff dynamics were well captured. The model generated very good simulations of the WT as indicated by the very good fit (NSE = 0.73). Subsequently, the transient model was run for summer 2016, 2017 and 2018 separately for both before and after restoration conditions. Hence, the outcomes of the numerical simulations were used to assess the effects of anthropogenic disturbance on the hydrological processes of the Eenokinneva catchment.

3.2.2. Surface runoff and water table depth before and after restoration

The three-dimensional distributed hydrologic model (HydroGeoSphere) generated significantly higher runoff amount under drained conditions than simulated under restored conditions in all of the three different summer rainfall situations (Figure 14, Figure 15 and Figure 16). This was clearly shown by the significantly large effect size index calculated for each year (Cohen's d = 0.95 for 2016; Cohen's d = 2.43 for 2017, Cohen's d = 2.51 for 2018). The effect is small, medium, and large when Cohen's d is between 0 and 0.20, 0.20 and 0.50, and greater than 0.50, respectively (Cohen, 1977). Furthermore, restoration moved the WT closer to the ground surface significantly (Cohen's d = 1.04 for 2016; Cohen's d = 2.73 for 2017, Cohen's d = 2.14 for 2018) than the WT level simulated under drained conditions (Figure 14, Figure 15 and Figure 16). A previous analytical study on the effects of similar restoration techniques on the WT dynamics also reported that restoration brought the WT closer to the ground surface (Menberu et al., 2016), which gives hope to future applications of numerical solutions to such problems. Such numerical applications can help to evaluate a variety of restoration techniques on paper before implementation and could save huge amounts of resources.

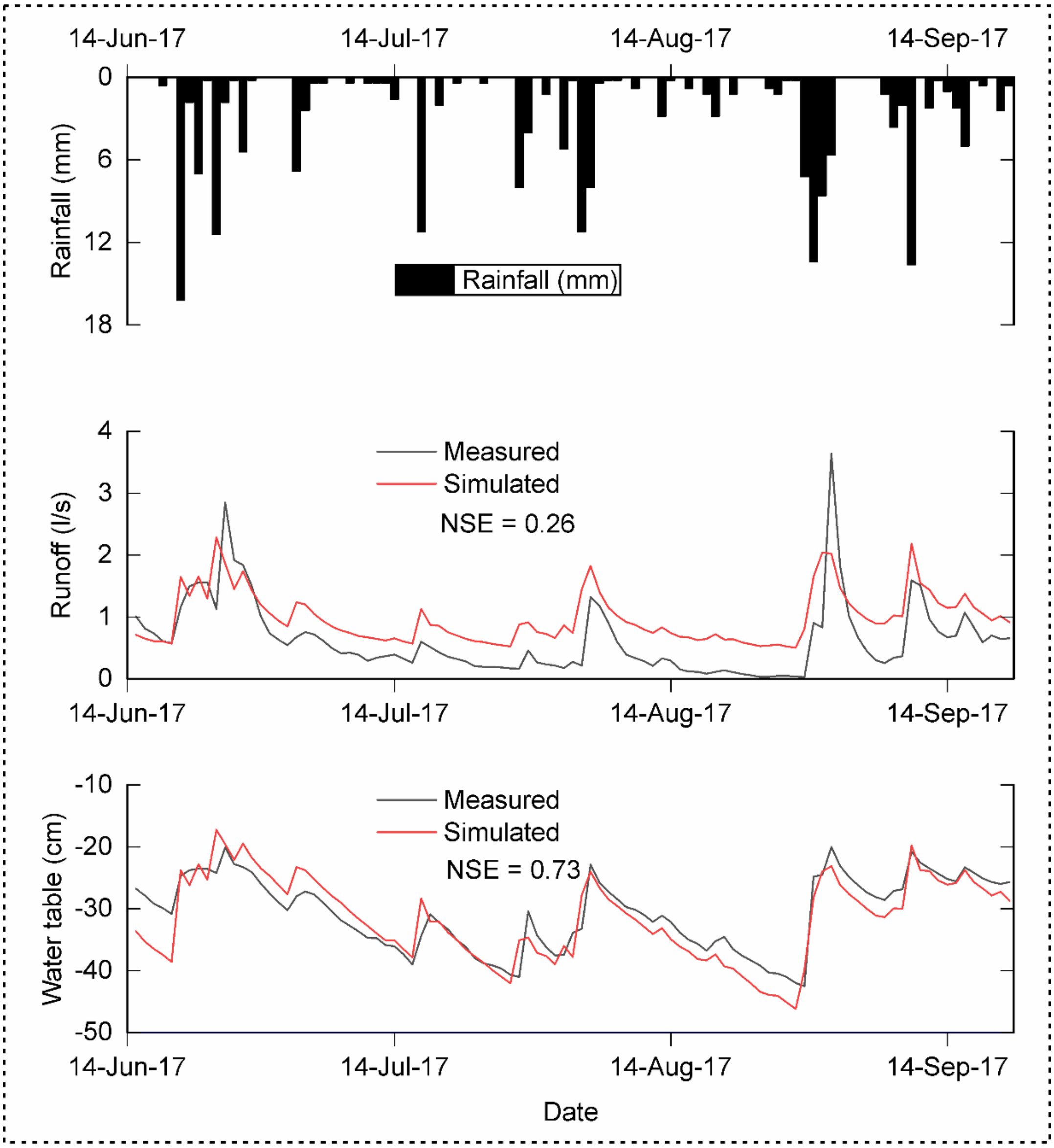

Figure 13. HydroGeosphere model performance showing ‘best fit’ between measured and simulated surface runoff and water table (measured at well_1) for forcing rainfall input. NSE is the Nash-Sutcliffe efficiency.

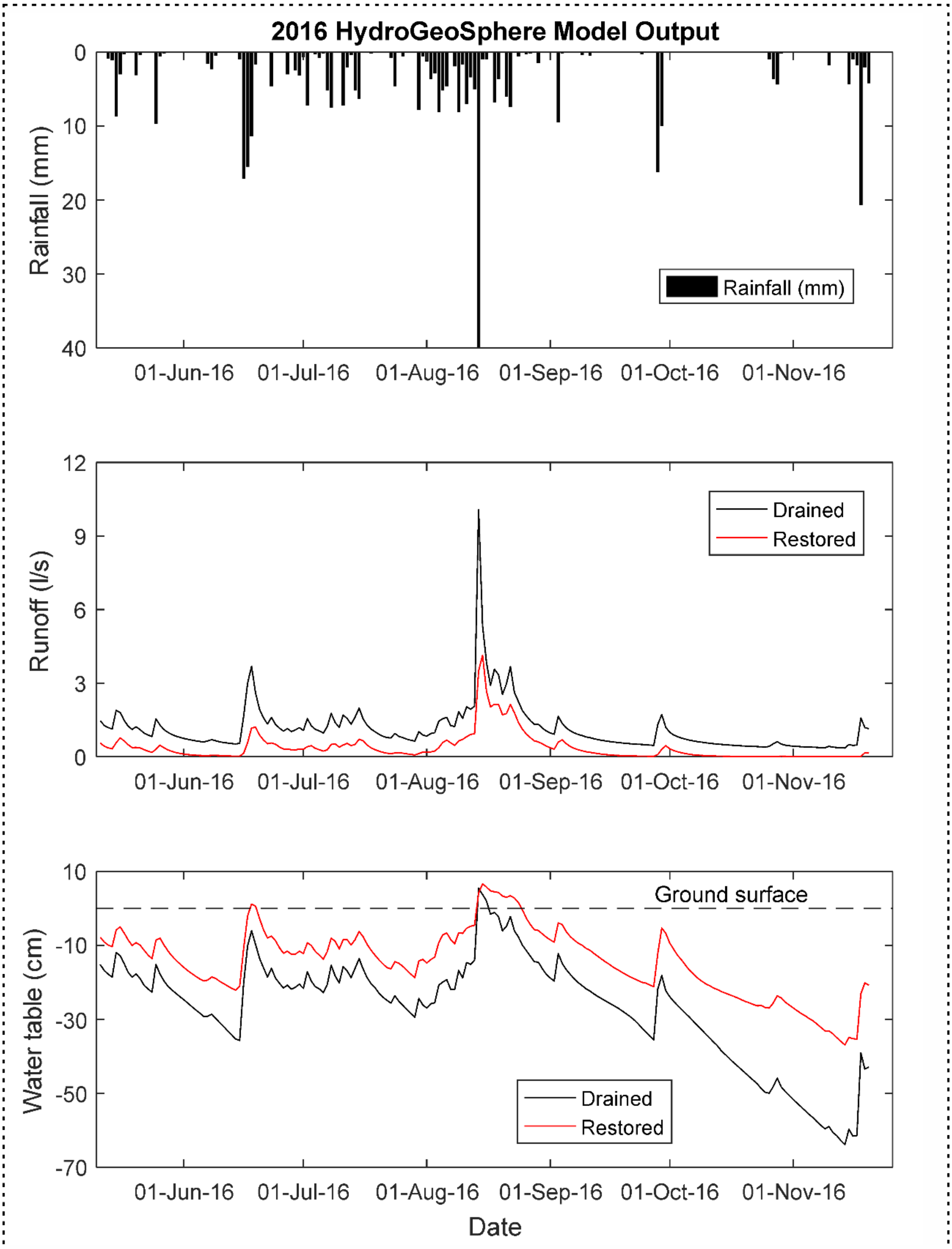

Figure 14. HydroGeosphere model simulations of runoff and water table for before and after restoration model conditions of 2016. Rainfall for 2016 taken from gridded data.

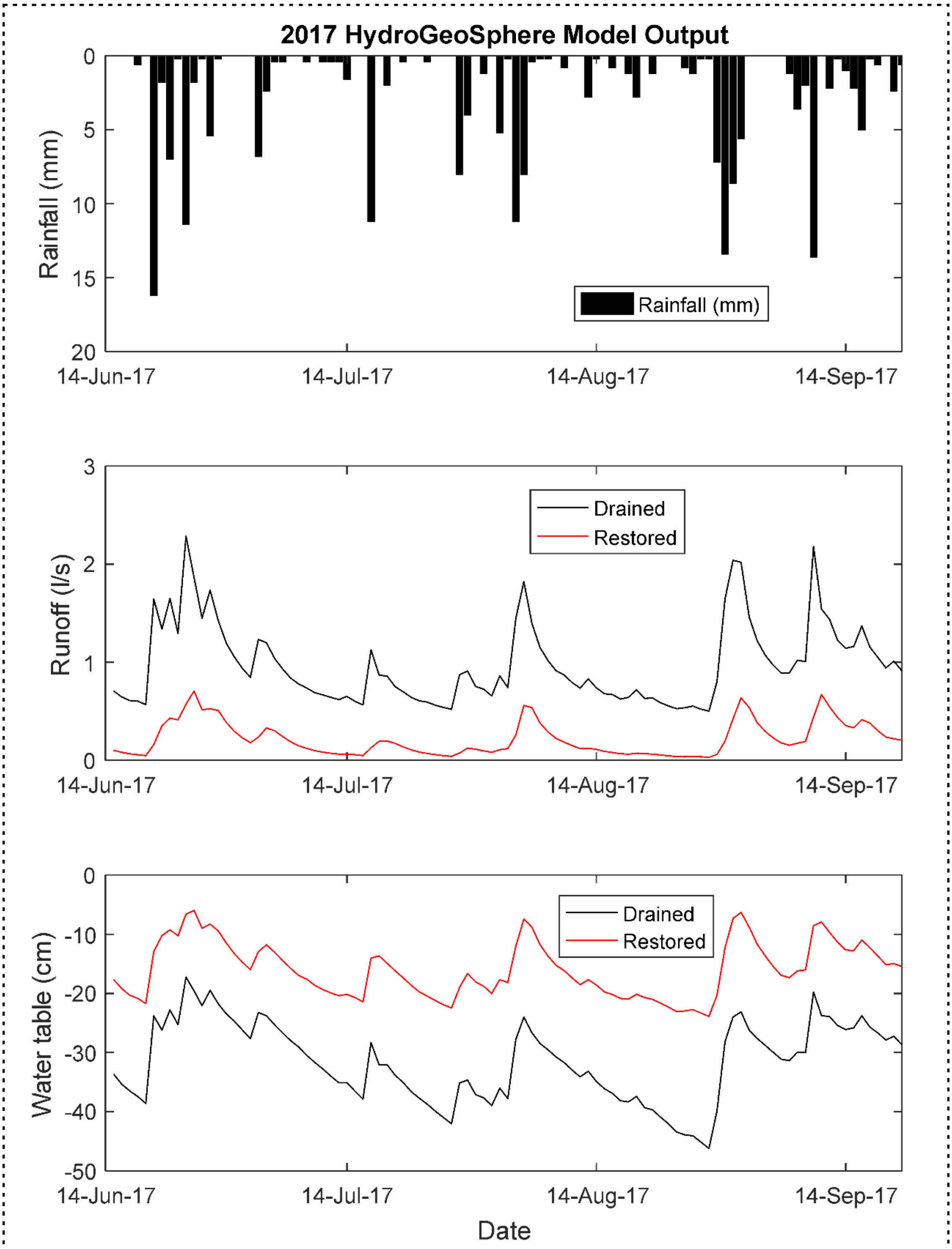

Figure 15. HydroGeosphere model simulations of runoff and water table for before and after restoration model conditions of 2017. Rainfall was measured on-site.

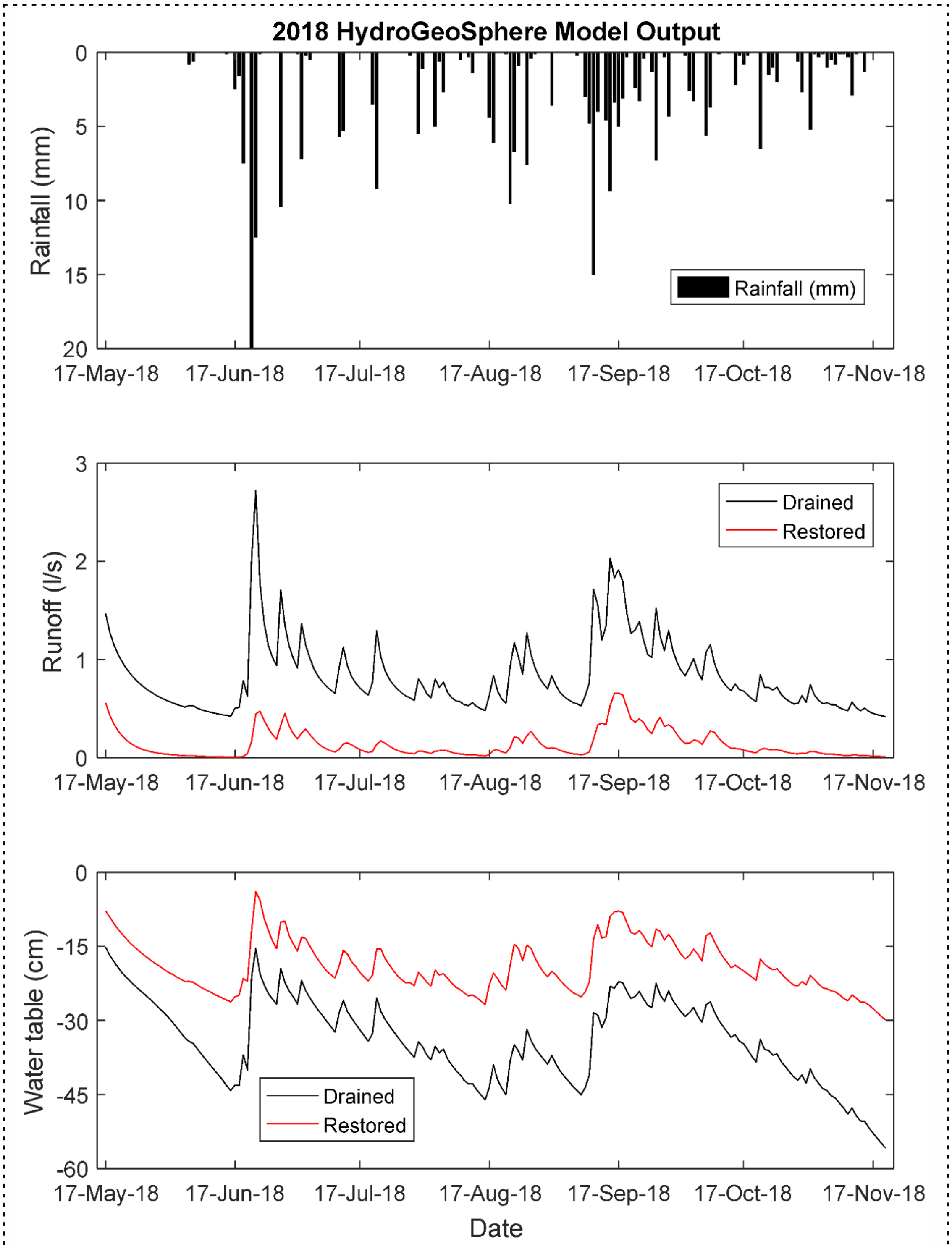

Figure 16. HydroGeosphere model simulations of runoff and water table for before and after restoration model conditions of 2018. Rainfall for 2018 taken from gridded data.

3.2.3. Spatiotemporal variability in water table depth and degree of saturation

The spatiotemporal variability in WT depth and degree of saturation showed clear hydrological differences between drained and restored condition (Figure 17, Figure 18).

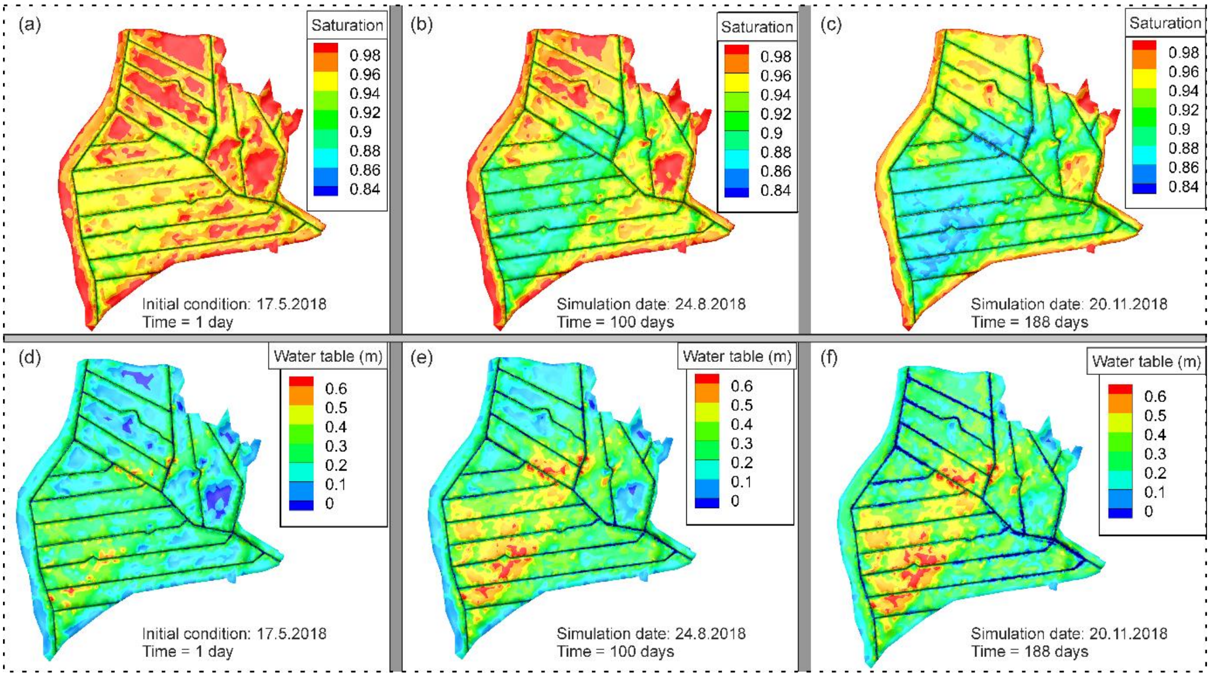

Figure 17. Snapshots of degree of saturation (top row) and water table depth (bottom row) showing model outputs for drained condition in 2018: (a, d) for the first day of simulation (day 1), (b, e) 100 days after start of simulation, and (c, f) 188 days after start of simulation.

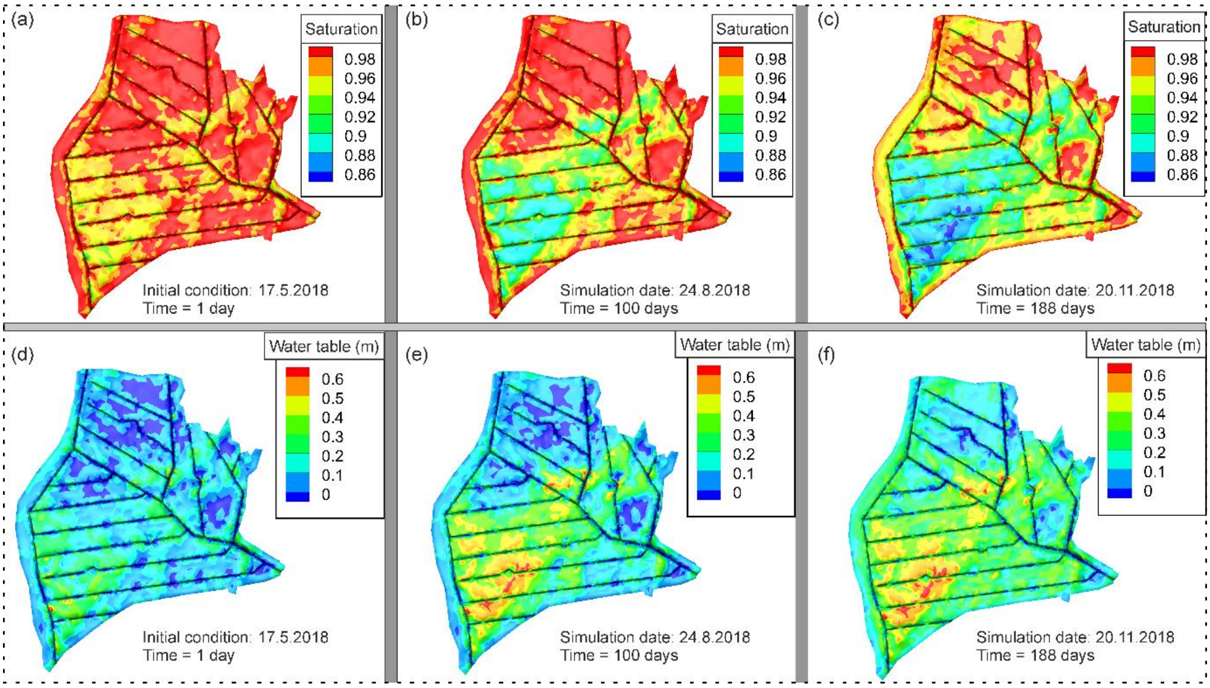

Figure 18. Snapshots of degree of saturation (top row) and water table depth (bottom row) showing model outputs for restored condition in 2018: (a, d) for the first day of simulation (day 1), (b, e) 100 days after start of simulation, and (c, f) 188 days after start of simulation.

At the beginning of the simulation (one day after steady state condition), the WT depth and degree of saturation for drained condition (before restoration) (Figure 17a, Figure 17d) clearly showed higher spatial variability than the restored condition (after restoration) (Figure 18a, Figure 18d). This has been the case 100 and 188 days after the start of simulation, although the degree of saturation and WT depth might decline over time depending on the weather conditions at the time of simulation. Before restoration, degree of saturation increased as distance from nearest ditches increases (higher spatial variability); however, after restoration the spatial variability of saturation slightly reduced. Similar properties, like that of the degree of saturation were also reflected in the WT dynamic. Furthermore, the WT depth significantly moved from deeper and lower hydraulic conductivity region of the peat layer (catotelm layer) observed before restoration to near ground surface, and higher hydraulic conductivity peat region (acrotelm layer) after restoration (Figure 14, Figure 15, Figure 16, Figure 17 and Figure 18). Similar model simulation outputs, which were interpreted as the results in 2018 (Figure 17 and Figure 18), also found for weather conditions recorded in 2016 and 2017 (Figure 14, Figure 15, Figure 16, Appendix A, Appendix B, Appendix C and Appendix D).

4. Conclusions

In this research project work, a two-year (frost-free period) before restoration and one year after restoration hydrological data was collected from Eenokinneva peatland catchment and analyzed thoroughly to assess the impacts of anthropogenic disturbance, such as drainage and following restoration, on peatland hydrology. However, a one year after restoration hydrological data was found not enough to assess drainage/restoration induced hydrological changes due to the unusual extreme continuous dry hydrological periods recorded in 2018. For project works that rely solely on analytical solutions, a one year after restoration hydrological data might not be enough to evaluate the subsequent hydrological changes; hence, we recommend continuing monitoring the hydrological data of such restored sites for at least a minimum of three years after restoration. However, in this study, a three-dimensional full-integrated surface-subsurface hydrological model using HydroGoesphere software (HGS) was developed to assess the impacts of artificial drainage and subsequent restoration on peatland hydrology. The 3D-model provided promising results and showed clear hydrological differences between drained and restored conditions of the model. Hence, in future, three-dimensional integrated surface-subsurface hydrological models could be used to evaluate/predict the impacts of a variety of restoration techniques (e.g., distance between peat-dams, length of dams, etc., can be optimized) on the hydrology of disturbed peatlands before its implementation. As well as changes in surface water groundwater interactions due to restoration could be useful to study by HGS modelling.

5. References

Ala-aho P, Rossi PM, Isokangas E, and Kløve B. (2015). Fully integrated surface–subsurface flow modelling of groundwater–lake interaction in an esker aquifer: Model verification with stable isotopes and airborne thermal imaging. *Journal of Hydrology*, *522*, 391-406. doi: https://doi.org/10.1016/j.jhydrol.2014.12.054.

Aquanty (2015). *HydroGeoSphere User Manual.* Aquanty Inc., Waterloo, Ontario, Canada.

Azous A and Horner RR (2000). *Wetlands and Urbanization: Implications for the Future.* CRC Press, Boca Raton, Florida.

Brunner P and Simmons CT. (2012). HydroGeoSphere: A Fully Integrated, Physically Based Hydrological Model. *Groundwater, 50*, 170-176.

Cherry JA (2012). Ecology of wetland ecosystems: water, substrate, and life. *Nature Education Knowledge*, *3*, 16.

Clarke D and Rieley J (2010). *Strategy for Responsible Peatland Management.* International Peat Society.

Cohen J (1977). CHAPTER 2 - the t test for means. In Jacob Cohen, *Statistical Power Analysis for the Behavioral Sciences (Revised Edition)*, pp. 19-74. Academic Press, New Jersey.

Dettmann U, Bechtold M, Frahm E, and Tiemeyer B. (2014). On the applicability of unimodal and bimodal van Genuchten–Mualem based models to peat and other organic soils under evaporation conditions. *Journal of Hydrology*, *515*, 103-115. doi: https://doi.org/10.1016/j.jhydrol.2014.04.047.

Finnish Meteorological Institute (2019). Year 2018 was warm and dry, *2019*(2/2019).

Greenup AL, Bradford MA, McNamara NP, Ineson P, and Lee JA. (2000). The role of Eriophorum vaginatum in CH4 flux from an ombrotrophic peatland. *Plant and Soil, 227*, 265-272.

Haapalehto TO, Vasander H, Jauhiainen S, Tahvanainen T, and Kotiaho JS. (2011). The Effects of Peatland Restoration on Water-Table Depth, Elemental Concentrations, and Vegetation: 10 Years of Changes. *Restoration Ecology*, *19*(5), 587-598. doi: 10.1111/j.1526-100X.2010.00704.x.

Healy RW and Cook PG. (2002). Using groundwater levels to estimate recharge. *Hydrogeology Journal*, *10*(1), 91-109. doi: 10.1007/s10040-001-0178-0.

Holden J, Chapman PJ, and Labadz JC. (2004). Artificial drainage of peatlands: hydrological and hydrochemical process and wetland restoration. *Progress in Physical Geography*, *28*(1), 95-123. doi: 10.1191/0309133304pp403ra.

Holden J, Palmer SM, Johnston K, Wearing C, Irvine B, and Brown LE. (2015). Impact of prescribed burning on blanket peat hydrology. *Water Resources Research*, *51*, 6472-6484.

Joosten H (2009). *The Global Peatland CO2 Picture: Peatland Status and Drainage Related Emissions in all Countries of the World.* Wetlands International, Netherlands.

Joosten H and Clarke D (2002). *Wise use of Mires and Peatlands.* International mire conservation group.

Koskinen M, Sallantaus T, and Vasander H. (2011). Post-restoration development of organic carbon and nutrient leaching from two ecohydrologically different peatland sites. *Ecological Engineering, 37*(7), 1008-1016. doi: 10.1016/j.ecoleng.2010.06.036.

Koskinen M, Tahvanainen T, Sarkkola S, Menberu MW, Laurén A, Sallantaus T et al. (2017). Restoration of nutrient-rich forestry-drained peatlands poses a risk for high exports of dissolved organic carbon, nitrogen, and phosphorus. *Science of The Total Environment, 586*, 858-869. doi: https://doi.org/10.1016/j.scitotenv.2017.02.065.

Krüger J, Leifeld J, Glatzel S, Szidat S, and Alewell C. (2015). Biogeochemical indicators of peatland degradation-a case study of a temperate bog in northern Germany. *Biogeosciences, 12*(10), 2861-2871. doi: 10.5194/bg-12-2861-2015.

Li Q, Unger AJA, Sudicky EA, Kassenaar D, Wexler EJ, and Shikaze S. (2008). Simulating the multi-seasonal response of a large-scale watershed with a 3D physically-based hydrologic model. *Journal of Hydrology, 357*(3), 317-336. doi: https://doi.org/10.1016/j.jhydrol.2008.05.024.

Marttila H and Kløve B. (2010). Managing runoff, water quality and erosion in peatland forestry by peak runoff control. *Ecological Engineering, 36*, 900-911.

McLaren R (2004). GRID BUILDER, a pre-processor for 2-D, Triangular element, finite-element programs. *Groundwater Simulation Group.University of waterloo, Waterloo, Ontario, Canada*.

Menberu MW, Haghighi AT, Ronkanen A, Marttila H, and Kløve B. (2018). Effects of Drainage and Subsequent Restoration on Peatland Hydrological Processes at Catchment Scale. *Water Resources Research, 54*, 4479-4497.

Menberu MW, Marttila H, Tahvanainen T, Kotiaho JS, Hokkanen R, Kløve B, and Ronkanen A. (2017). Changes in Pore Water Quality After Peatland Restoration: Assessment of a Large-Scale, Replicated Before-After-Control-Impact Study in Finland. *Water Resources Research, 53*, 8327-8343.

Menberu MW, Tahvanainen T, Marttila H, Irannezhad M, Ronkanen A, Penttinen J, and Kløve B. (2016). Water-table-dependent hydrological changes following peatland forestry drainage and restoration: Analysis of restoration success. *Water Resources Research, 52*, 3742-3760.

Paavilainen E and Päivänen J (1995). *Peatland Forestry: Ecology and Principles.* vol. 111, Springer-Verlag Berlin Heidelberg, Berlin.

Pirinen P, Simola H, Aalto J, Kaukoranta J, Karlsson P, and Ruuhela R. (2012). Climatological statistics of Finland 1981–2010. *Finnish Meteorological Institute Reports, 1*, 83.

Schwarzel K, Simunek J, Stoffregen H, Wessolek G, and van Genuchten MT. (2006). Estimation of the unsaturated hydraulic conductivity of peat soils: laboratory versus field data. *Vadose Zone Journal, 5*, 628-640.

Strack M (2008). *Peatlands and Climate Change.* IPS, International Peat Society, Jyväskylä.

Tecplot I (2013). Tecplot 360 User's Manual Release 1.

Turunen J (2008). Development of Finnish peatland area and carbon storage 1950-2000. *Boreal Environment Research, 13*(4).

Wu J, Kutzbach L, Jager D, Wille C, and Wilmking M. (2010). Evapotranspiration dynamics in a boreal peatland and its impact on the water and energy balance. *Journal of Geophysical Research: Biogeosciences, 115,* G04038. doi: 10.1029/2009JG001075.

Yu Z, Beilman DW, Frolking S, MacDonald GM, Roulet NT, Camill P, and Charman DJ. (2011). Peatlands and Their Role in the Global Carbon Cycle. *Eos, Transactions American Geophysical Union, 92*, 97-98.

6. Appendices

Appendix A: Eenokinneva catchment HydroGeosphere simulation outputs under drained conditions of the model for daily gridded rainfall in 2016.

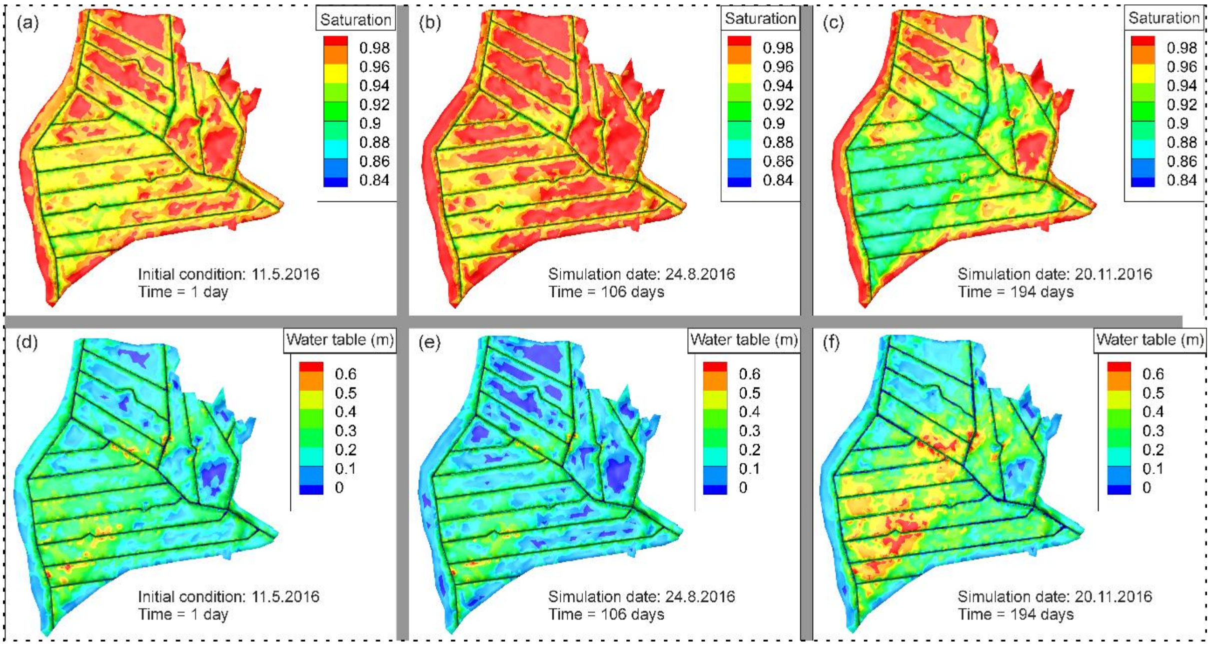

Appendix B: Eenokinneva catchment HydroGeosphere simulation outputs under restored conditions of the model for daily gridded rainfall in 2016.

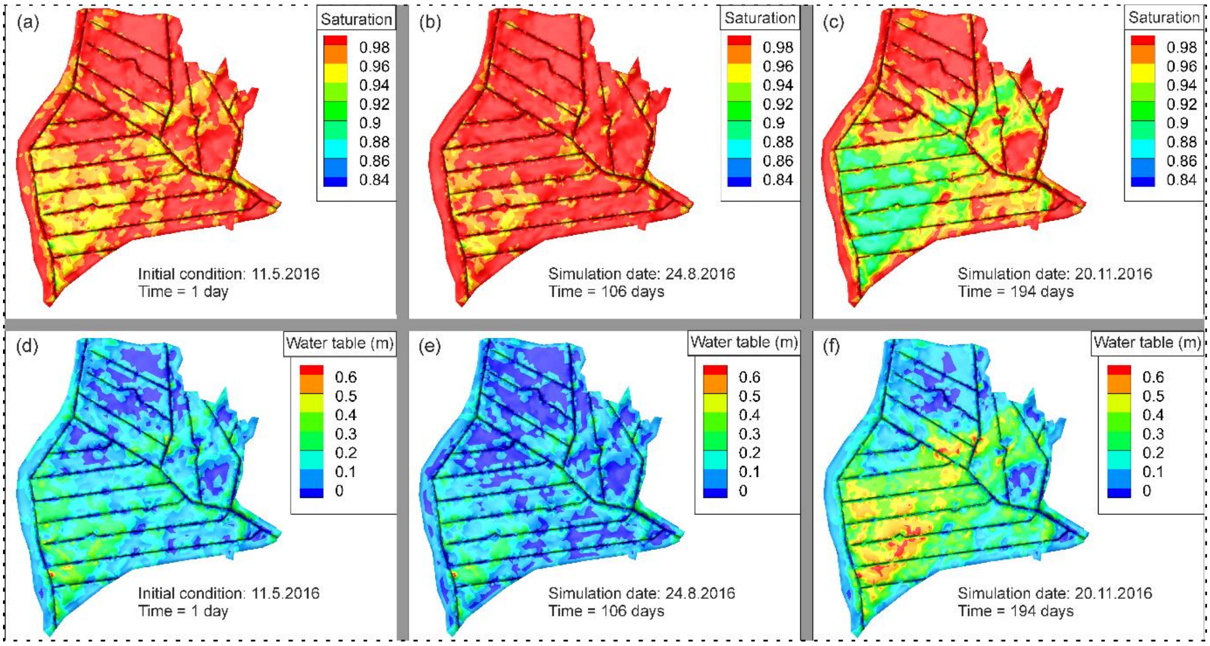

Appendix C: Eenokinneva catchment HydroGeosphere simulation outputs under drained conditions of the model for daily rainfall recorded in 2017.

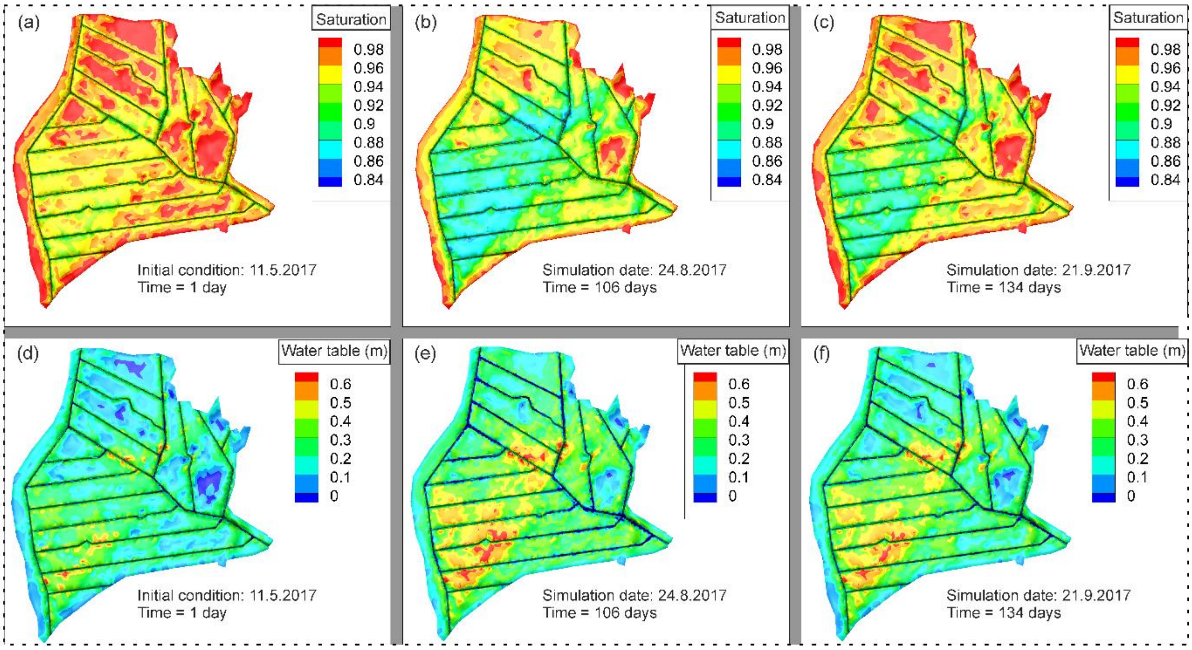

Appendix D: Eenokinneva catchment HydroGeosphere simulation outputs under restored conditions of the model for daily rainfall recorded in 2017.